Shielding effect in pile groups adjacent to deep unbraced and braced excavations

Ravintharakumaran Nishanthan, D. S. Liyanapathirana & Chin Jian Leo

Published online: 08 Jul 2016.

Submit your article to this journal

Article views: 3

View related articles

View Crossmark data

Shielding effect in pile groups adjacent to deep unbraced and braced excavations

Ravintharakumaran Nishanthan, D. S. Liyanapathirana* and Chin Jian Leo

This paper investigates the shielding effect within piles in a group adjacent to deep unbraced and braced excavations. Numerical simulations based on the finite element method are performed on free-head and capped-head piles in three different pile group configurations. The numerical model is validated by simulating a series of centrifuge tests. The problem was modelled considering the three-dimensional geometry, which facilitates to simulate the shielding effect of piles within the group during an excavation. Results show that the presence of front piles near the excavation face reduces the detrimental effects on the rear piles within the group in unbraced excavations. In addition, the provision of a pile cap significantly reduces the deflection of pile group in unbraced excavations due to load transfer to rear piles, which are located away from the excavation. However, in braced excavations, unless the excavation is deep, the shielding effect and the presence of a pile cap are less significant on the pile group behaviour.

Introduction

Deep excavations in congested urban areas are inevitable for the construction of basements, mass rapid transit stations and other underground facilities. During the excavation, due to the stress release in the adjacent soil, the confining pressure around existing nearby pile foundations tends to reduce drastically and finally induce additional deflections and bending moments. It is important to quantify these detrimental effects and understand the shielding effect within pile groups in order to design the most effective and economical excavation support systems to protect the existing structures during nearby deep excavations.

Both numerical and experimental studies have been carried out extensively in the last few decades to investigate the significance of ground deformations on single pile response during nearby excavations. However, only few research studies have been carried out in the literature investigating pile group behaviour due to excavation-induced ground deformations and shielding effect within pile groups (Chen and Poulos 1996; Leung et al. 2003; Ong et al. 2009). Ng et al. (2005), Huang et al. (2009) and Liang et al. (2013) also discussed shielding effect within pile groups due to ground movements in general but not considering the ground deformations due to open excavations as considered in this research or with braced excavations.

Chen and Poulos (1996) studied the shielding effect in pile groups due to braced excavation-induced lateral movements using finite element and boundary element approaches. Pile group behaviour is investigated by applying free field ground deformations from a finite element analysis to the piles, using the program PALLAS (Hull 1987), which is based on the

boundary element method. They introduced a group factor expressing the shielding effect, which is defined as the ratio between the pile response when it is part of a pile group and pile response when it is an isolated single pile at the same location. According to Chen and Poulos (1996), the shielding effect is not significant for shallow excavations. For deep excavations with larger soil movements, where stability number, N, is greater than 6 and pile–soil lateral pressure reaches its ultimate value, shielding effect has a substantial influence based on the configuration of piles within the group. Stability number N is given by,
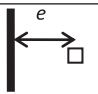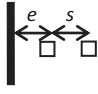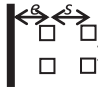
$$N = \frac{\gamma H}{c_{\mathrm{u}}} \tag{1}$$

where γ is the unit weight of soil, H is the depth of the excavation and c_{u} is the undrained shear strength of the soil.

Leung et al. (2003) and Ong et al. (2009) investigated the shielding effect in sandy and clayey soils, respectively, using centrifuge tests. They investigated the behaviour of free-head and capped-head pile groups made of two, four and six piles located behind unbraced excavations. According to their results, when the piles are located in a row parallel to the wall, the effect of pile–soil–pile interaction on the behaviour of individual piles is insignificant compared to the case with piles positioned perpendicular to the wall. In the latter case, the front piles located closer to the retaining wall reduced the adverse effects of excavation-induced soil movement on rear piles. Furthermore, provision of a pile cap significantly affects the behaviour of individual piles in the front row, experiencing high lateral movements. In addition, it was found that peripheral piles in a group experience higher bending moments when compared to interior piles of the same group, which are less exposed to the adverse effects of excavation-induced ground movements. They mentioned that since the pile caps are transmitting the

School of Computing, Engineering and Mathematics, University of Western Sydney, Locked Bag 1797, Penrith, NSW 2751, Australia

*Corresponding author, email s.liyanapathirana@uws.edu.au

Table 1   Pile configurations used in the analysis

Pile configurations	Test no	Geometric parameters	Pile head condition
e	T1	e=3 m	Free-head
	T2	e=5 m	Free-head
e s	T3	e=3 m, s=2 m	Free-head
	T4	e=3 m, s=2 m	Capped-head
e s s	T5	e=3 m, s=2 m	Free-head
	T6	e=3 m, s=2 m	Capped-head
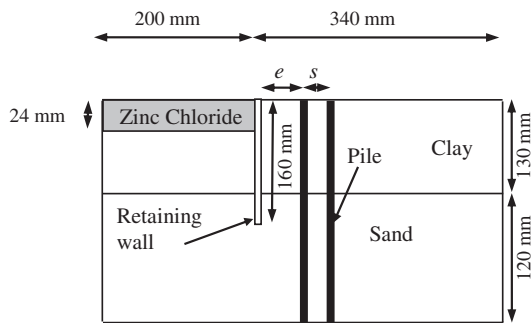
1   Centrifuge model arrangement with unsupported wall (Ong et al., 2006)

Note: e – distance between Freon pile and excavation wall,

s – spacing between piles

bending moments from front piles to rear piles, the design of pile caps significantly contributes to the degree of shielding within piles in a group during nearby excavations.

Response of pile groups subjected to excavation-induced ground movements is a three-dimensional problem due to the soil flow between adjacent piles and the wall supporting the excavation. In addition, the pile and ground deformations are coupled in the real situation. Although two-step approaches discussed before decouple ground deformations and pile deformations, this assumption is not realistic. The coupled finite element studies found in the literature investigating pile group behaviour during nearby excavations modelled piles in a group using equivalent walls and analysed considering plane strain geometry (e.g. Finno et al. 1991). However, the investigation of pile group behaviour including the shielding effect during nearby excavations including the full three-dimensional geometry of the excavation and pile group is important. Another significant aspect, which needs to be included, is the pile–soil interaction incorporating separation at the pile–soil interface.

Hence, the main aim of this paper is to investigate the pile group behaviour due to lateral ground deformations caused by nearby braced and unbraced excavations with special emphasis on shielding effects within the group considering the three-dimensional geometry, pile–soil interaction and the separation at the pile–soil interface. A braced excavation is also considered instead of an unsupported wall similar to most previous studies

because in soft clay soils, struts are used to support the wall during the excavation. Soil anisotropy effects, important for predicting settlements behind the wall, are not incorporated in this analysis to minimise the number of parameters associated with constitutive model describing soil behaviour. This approach is reasonable because in this study, shielding effect is investigated predominantly based on the lateral behaviour of piles (maximum lateral deformation and bending moment) during a braced excavation and not based on the settlements. In the modified cam-clay (MCC) model used to simulate the behaviour of soft clay, shear modulus is varied with the strain level. Centrifuge tests reported by Ong et al. (2009) were modelled using the three-dimensional finite element models to validate the numerical model used for the parametric study. Next, a parametric study is carried out to investigate the shielding effect of piles in a group during a deep braced excavation, varying pile group configuration and head conditions. Finally, the degree of shielding was investigated during deep braced excavations considering the maximum bending moment of piles in a group with respect to the behaviour of a single pile at the same location.

Model calibration

Description of the centrifuge test

Pile configurations used in centrifuge tests by Ong et al. (2009) as shown in Table 1 are used to calibrate the numerical model. In these tests, the behaviour of a pile group adjacent to an unbraced excavation is studied. Figure 1 shows the centrifuge set-up used for the investigation of shielding effect within pile groups. The model container has dimensions of 540 mm × 200 mm × 470 mm. The Kaolin clay was filled up to a depth of 130 mm above a Toyoura sand layer, which has a thickness of 120 mm. Latex bag filled with $ZnCl_2$ solution, which has a unit weight equivalent to the clay, is used to represent the soil region that needs to be excavated. Hollow square aluminium tubes with outer width of 12.6 mm are used to model the piles. Tests were carried out at a centrifugal acceleration of 50 g at the geotechnical centrifuge facility, National University of Singapore. Here, the 24-mm-deep excavation was carried out by draining the $ZnCl_2$ solution in six steps over 140 s and the test is continued to complete the consolidation over 2 h in the model scale. According to scaling laws adopted in centrifuge
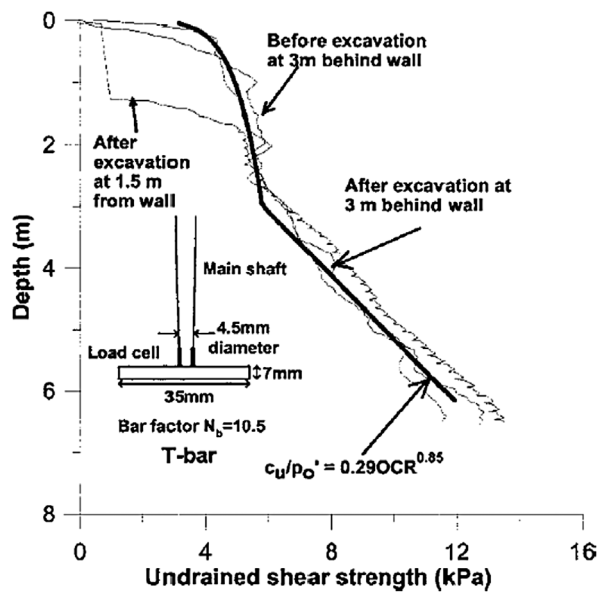
2   Variation of undrained shear strength with depth (Ong et al. 2006)
Source: American Society of Civil Engineers
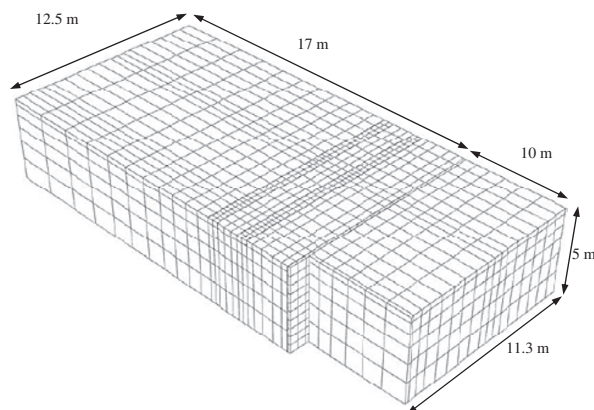
3   Finite element mesh used for the modelling of Test 3

modelling, all dimensions must be multiplied by the acceleration level of the test to get the prototype dimensions of the model set-up. Since the problem is related to consolidation, time taken for the excavation and consolidation in model scale should be multiplied by the square of the centrifuge acceleration. Therefore, in the prototype scale, the width of the square pile is 630 mm and the excavation depth is 1.2 m. The 1.2-m-deep excavation is carried out over 2 days and the overall analysis time is 310 days.

Material models and properties

The finite element analysis simulating the centrifuge test was carried out assuming the undrained behaviour for clay because only the distribution of undrained properties is available for the clay used for the centrifuge tests. Since the clay has a permeability of 1.36×10^{-3} m/day and the excavation was carried out

in two days, this is a reasonable assumption. The stress–strain behaviour of clay used for the centrifuge test was simulated using the Mohr–Coulomb criteria. Mohr–Coulomb model with linear elasticity is not suitable to predict the ground surface settlements or pile settlements due to ground heave predicted near the wall (Potts and Zdravkovic 2001). However, in this case, finite element predictions for pile lateral deformations and bending moments are compared with those recorded during the centrifuge test. Therefore, it is reasonable to use the Mohr–Coulomb model for this analysis.

The variation of undrained shear strength of the clay with depth is shown in Fig. 2. The top 2.5-m soil crust was found to be over consolidated and soil below that level was normally consolidated. The elastic modulus of the Kaolin clay was calculated using $E_c/c_u = 400$ (Poulos and Davis, 1980). The internal friction angle and the Poisson's ratio for the undrained Kaolin clay were assumed as 0 and 0.49, respectively. Lateral earth pressure coefficient at rest, K_o, is taken as one. The unit weight of the soil is 16.5 kN/m³ (Ong 2004). The Toyoura sand layer below the clay layer was also modelled using the Mohr–Coulomb model with an internal friction angle of 40° and an elastic modulus of $6z$ MPa, where z is the depth below the ground surface in meters (Ong et al. 2006). The Poisson's ratio of the sand is assumed to be 0.3.

Hollow square aluminium tubes are used as piles. Bending stiffness of each pile is 2.2×10^5 kNm² in prototype scale, which is equivalent to the stiffness of a 600-mm-diameter concrete pile with an embedment depth of 12.5 m. A 3-mm-thick aluminium plate is used as the wall in the centrifuge test, with prototype bending stiffness of 24×10^3 kNm²/m, which is equivalent to a steel sheet pile wall with an embedment depth of 8 m. Piles, pile cap and wall are modelled assuming the linear elastic behaviour.

Finite element modelling

A three-dimensional finite element model based on prototype dimensions is used to simulate the centrifuge tests. ABAQUS/Standard (2013) finite element program is used to investigate the problem. Due to symmetry of the problem, only half of the geometry is considered for the numerical model as shown in Fig. 3. Non-linear geometry of the problem is taken into account during the analysis by activating the NLGEOM command in ABAQUS/Standard (2013).

Soil, pile, pile cap and wall were modelled using 20-node quadrilateral brick elements with reduced integration formulation. At the bottom of the finite element mesh, horizontal and vertical movements are restrained ($u_x = u_y = u_z = 0$). Nodes over the vertical side faces are free to move in the vertical and horizontal directions along the surfaces of the container and restrained only in the directions perpendicular to the side faces. In the centrifuge model, tips of the pile group extend up to the bottom of the container and the movement of pile tips is restrained only by the surrounding soil and base of the container. If the same restraining conditions are applied to pile tips as for the base of the container, large bending moments will be developed at pile tips, which is not in agreement with the observed bending moments at the pile tip. Hence, only the centre of the bottom of each pile is restrained from movements in all directions.
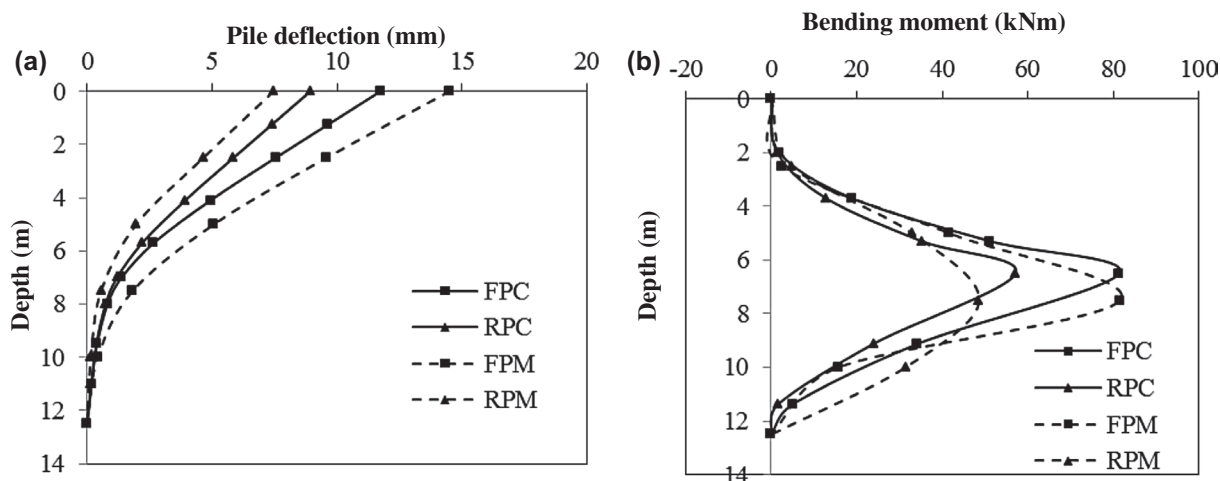
4 *a* Pile deflection and *b* bending moment for test T3
Notes: FPC – computed value for front pile, RPC – computed value for rear pile, FPM – measured value for front pile and RPM – measured value for rear pile

The soil–pile interaction in tangential direction is modelled using the Coulomb friction model, which is governed by a friction coefficient and a limiting displacement for elastic slip. Here, a value of 0.3 was selected as the friction coefficient. Based on the typical values reported by Broms (1979), a limiting displacement of 5 mm was selected for the elastic slip to mobilise the full skin friction at the pile–soil interface based on the typical values reported by Broms (1979). The pile–soil interaction in normal direction is modelled allowing separation at the pile–soil interface. Another advantage of allowing slippage and separation at the pile–soil interface is that it will avoid the overestimation of the deflection and bending moment of the pile as shown by Miao et al. (2006).

Another important point to be noted when selecting interface friction coefficient and elastic slip is the size effects in model and prototype cases at the soil–pile interface. According to Balachowski (2007), size effects are important in model and prototype comparisons only if pile diameter to average grain size ratio is less than 20 in 30–100-g centrifuge acceleration levels. In this case, soft Kaoline clay, which has fine particles, is used. Hence, size effects are not significant for the model and prototype scales used for the finite element analysis. However, in this case, computed lateral pile deformations are prominent compared to pile settlements. Hence, the magnitude of elastic slip and friction coefficient does not have a significant influence on the pile lateral deformations and bending moments.

## Validation of finite element model with centrifuge test data

In this section, validation of the adopted finite element model to investigate shielding effect of pile groups is presented. Validation was carried out using centrifuge tests T3 and T5 as shown in Table 1 with groups of two piles in a row perpendicular to the wall and four piles, respectively. Figure 4 shows the computed and measured pile responses for the test T3 at the end of 1.2-m depth of excavation. Two free-head piles are used in this test. The front pile is located 3 m

away from the excavation and the rear pile is located 5 m away from the excavation. Since the centrifuge test used an unbraced excavation, pile deformations shown in Fig. 4(a) are in cantilever shape. Deflection of front pile, obtained from the finite element analysis, is slightly under predicted and the deflection of rear pile is slightly over predicted compared to the centrifuge test results. This may be due to the inhomogeneous shear strength parameters in the lateral direction of the soil domain used for the centrifuge test as illustrated in Fig. 2. Measured undrained shear strengths show different profiles at distances of 1.5 and 3 m from the excavation after completion of the excavation.

The predicted bending moment profile for the front pile shown in Fig. 4(b) agrees well with the measured values during the centrifuge test. However, for the rear pile, computed bending moment slightly over predicted the measured bending moment. In both piles, the maximum bending moment occurs near the mid-height of the pile. Pile deflections and bending moments developed in the rear pile are less than those developed in the front pile. The maximum bending moment developed in the rear pile is 30% less than that in the front pile and the maximum deflection developed in the rear pile is 24% less than that in the front pile. These results confirm the shielding effect of front piles on the rear piles.

Figure 5 shows the measured and predicted responses for a group of 2 × 2 free-head piles (T5) and they are similar to the results given by test T3. In test T5, two piles are located in a row perpendicular to the wall as shown in Table 1. The predicted location of the maximum bending moment slightly differs from the measured one. Due to the arching effect between piles in a row parallel to the wall, the pile deflection and bending moment values are slightly less for test T5 when compared to test T3. This difference becomes significant when the ratio of pile spacing over pile diameter decreases and this will be discussed later. Overall, finite element predictions agree well with the measured pile deflections and bending moments.

Centrifuge tests T3 and T5 consist of free-head pile groups. When there is a capped pile group, a concrete pile cap with

Pile deflection (mm)
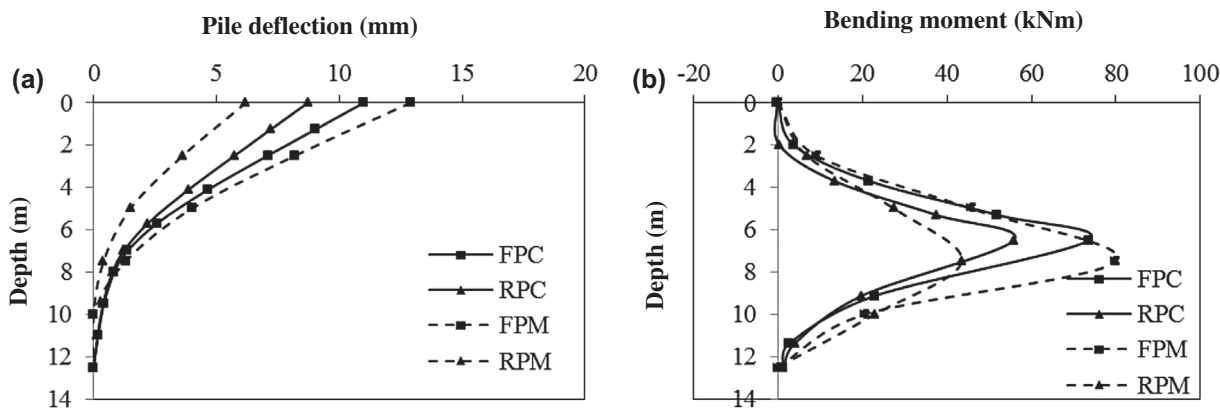
Bending moment (kNm)

5 *a* Pile deflection and *b* bending moment for test T5
Notes: FPC – computed value for front pile, RPC – computed value for rear pile, FPM – measured value for front pile and RPM – measured value for rear pile

Bending moment (kNm)
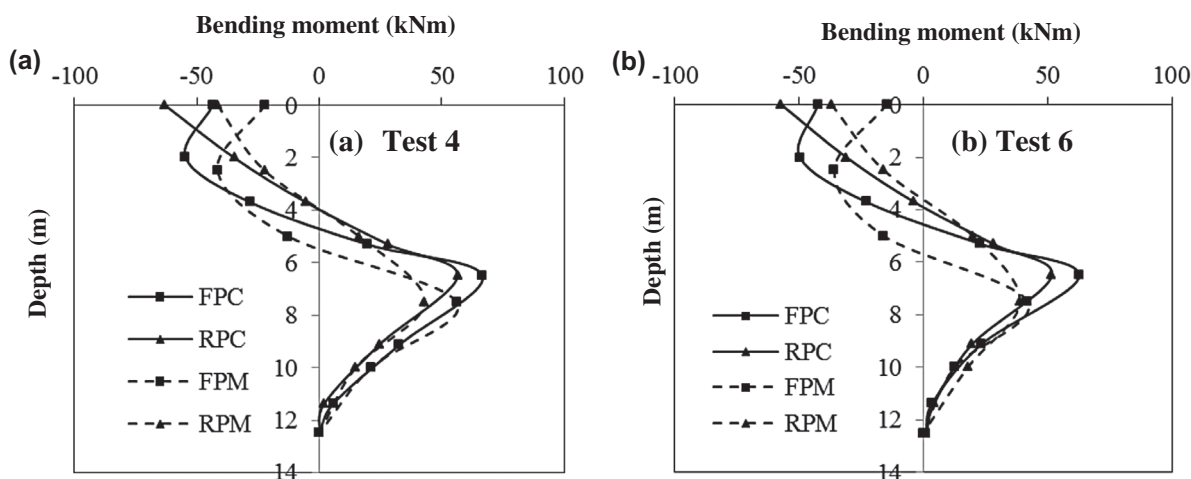
Bending moment (kNm)

6 Pile bending moment for *a* Test 4 and *b* Test 6
Notes: FPC – computed value for front pile, RPC – computed value for rear pile, FPM – measured value for front pile and RPM – measured value for rear pile

planar dimensions of 3 m × 1.25 m and a thickness of 1.55 m is used for test T4 and 3 m × 3 m cap with thickness of 1.55 m is used for test T6. Figure 6 shows the bending moment distributions along the piles predicted from the finite element model and the bending moment measured during the centrifuge test for T4 and T6. Bending moment predictions from the finite element model are slightly higher than the centrifuge test results. One reason for this difference may be the method adopted to connect the concrete pile cap to the pile group. In the centrifuge test, pile cap is welded to the pile group and in the finite element model, a tie constraint is used to connect the cap to the pile, which represents a fixed boundary condition with zero rotational and translational movements at the pile head. The difference between the degrees of restraint in two cases may have contributed to the difference observed between finite element and centrifuge results. However, the overall bending moment distribution has the same shape. Therefore, in the next section, shielding effect within pile groups is discussed using finite element results obtained from the same numerical model.

Shielding effect in pile groups adjacent to unbraced excavations

Figures 7 and 8 show the comparison of pile head deflection and maximum bending moment, respectively, for rear and front piles in tests T3 and T5 with free-head piles and T4 and T6 with capped-head piles. In these two figures, results are also presented for single piles at the corresponding locations for front and rear piles, which are located at 3 m (T1) and 5 m (T2) from the excavation. For tests T4 and T6 with pile caps, bending moment developed at the pile head is negative. Hence, both maximum positive and negative moments are given.

According to Fig. 7, minimum pile deflections are observed when there is a pile cap (T4 and T6). This is due to the high stiffness of the pile cap. The maximum pile head deflection is the same for both front and rear piles. In this case, pile tip is pinned. Therefore, both piles show the same deformed shape and do not show any shielding effect from the front pile on the rear pile. For tests T3 and T5 with free-head piles, front and
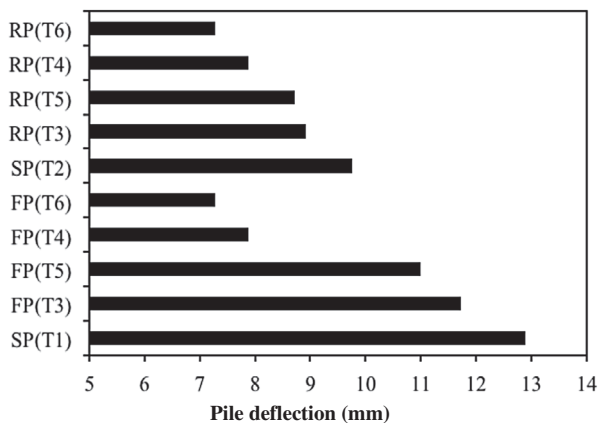
7 Comparison of pile head deflection (unbraced excavation)
Notes: SP – single pile, FP – front pile and RP – rear pile

rear piles deflect slightly less than single piles at 3 and 5 m away from the wall, respectively. The reduction in deflection in front pile compared to the single pile at the same location is due to the contribution from the rear pile in carrying extra loads imposed on the pile group by excavation-induced ground deformations. In both tests, T3 and T5, rear piles deform less due to the shielding effect from the front piles. When the number of piles in the group increases from 2 to 4, pile deflection is further decreased. These observations confirm that the presence of more piles tends to increase the shielding effect on the pile group. In this section, only 2-m spacing between piles is considered. However, the ratio between pile spacing and diameter may have a significant influence on the shielding effect of the pile group. This will be investigated in detail in a later section.

Maximum bending moments for the same set of tests also show a response similar to deflections. When the number of piles increased from 2 to 4, maximum bending moment reduces due to increased shielding effect of the pile group for both free-head and capped-head pile groups. In capped pile groups, maximum negative bending moment is less than maximum positive

bending moment for front piles, but in rear piles, maximum negative bending moment is higher than maximum positive bending moment. Overall, maximum bending moments developed in front and rear piles in capped- and free-head piles are less than those developed in single piles at the corresponding locations, confirming the shielding provided by the piles in a group.

Parametric study for braced excavations
Scope of the study

In the previous section, the shielding effect of pile groups is investigated for unbraced excavations. In this section, a parametric study is carried out to investigate the shielding effect of pile groups adjacent to deep braced excavations in clayey soils. The braced excavation is carried out in normally consolidated stiff Boston Blue Clay. Three different pile configurations were considered in the parametric study similar to the previous centrifuge tests but for a braced excavation. The soil properties were extracted from Hashash (1992) as shown in Table 2. The stiff clay was modelled using the Modified Cam-Clay model, which has different stiffnesses for loading and unloading stress conditions. Generally, the non-linear small strain behaviour of the shear modulus has a significant influence on the vertical settlements of the wall and retained soil during excavations. Therefore, void ratio of the soil is changed in the material sub-routine considering the strains developed in each time step of the analysis. Then, the shear modulus is computed considering these void ratios. Hence, the shear modulus used for the simulations is not a constant when the soil is in the elastic region.

The excavation is supported by a 40-m-long and 1-m-thick diaphragm wall, as shown in Fig. 9. The square piles in the group are 25-m long and the side width of each pile is 0.5 m. The wall and the piles are made of concrete, which has a Young's modulus of 40 GPa. The finite element model used for the parametric study is extended five times the width of the pile group measured from the centre of the pile group in the horizontal transverse direction, which is the direction perpendicular to the side view shown in Fig. 9. In the vertical
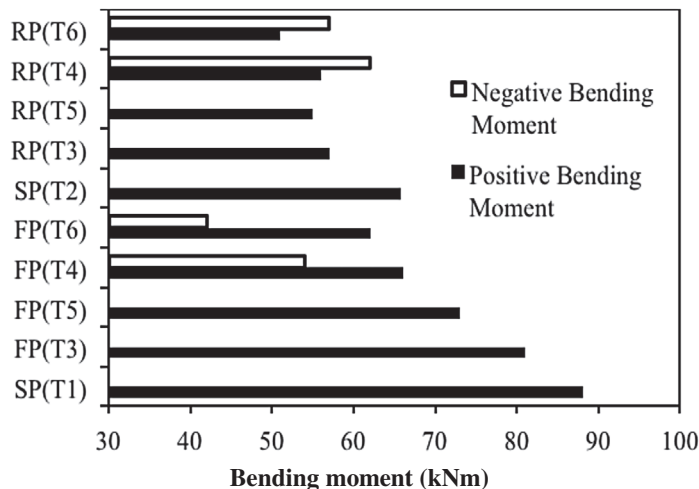

8 Comparison of maximum bending moment (unbraced excavation)
Notes: SP – single pile, FP – front pile and RP – rear pile

Table 2 Soil parameters used in the analysis

Soil parameters	Symbol	Value
Unit weight (kN/m³)	γ	18.0
Void ratio	e	1.0
Poisson's ratio	v	0.27
Stress ratio	M	1.1
Log plastic bulk modulus	λ	0.184
Log elastic bulk modulus	κ	0.034
Lateral earth pressure coefficient	K_0	0.53
Permeability (*m*/day)	k_x, k_y	1×10^{-5}
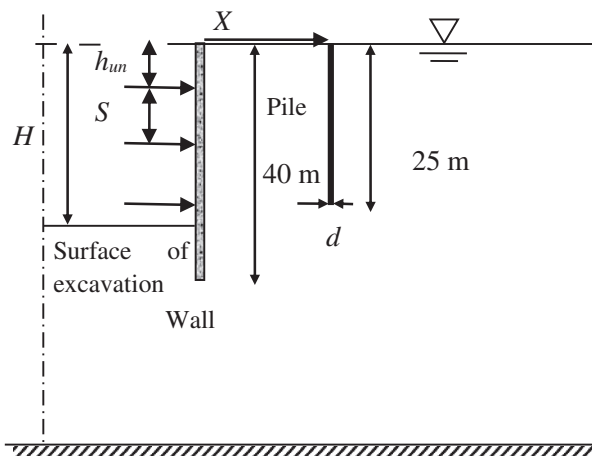
9 Side view of the excavation used in the three-dimensional finite element analysis
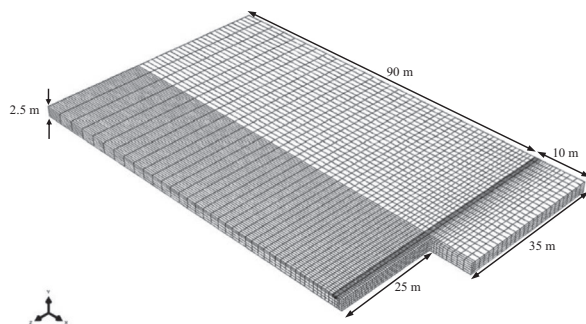
10 Finite element mesh used for the modelling of single pile located 1.5 m (three pile diameters) from the excavation face

direction, finite element model extends a distance 1.4 times the final depth of the excavation, measured from the bottom of the final excavation level. The finite element model extends four times the depth of excavation, measured from the centre of the excavation in the longitudinal direction (*X* direction shown in Fig. 9). Since these boundaries are placed far away from the pile group, they will avoid boundary effects on the pile group response. Figure 10 shows the finite element mesh used for the modelling of a single pile located 1.5 m (three pile diameters) from the excavation face.

The bracing system is modelled using one-node spring elements. A simple construction sequence is used in the analysis

as shown in Fig. 9. Soil elements were removed up to a depth of h_{un} and the first row of struts is installed at the level of the newly excavated surface. Then, the excavation proceeds up to a depth of $(h_{un} + S)$ and the second strut is installed at the level of the newly excavated surface. Inside the excavation, the water table is maintained 2 m below the newly excavated surface to simulate the lowering of water table due to pumping inside the excavation. Also, this helps overcome convergence problems associated with finite element modelling of excavations. For the soil behind the excavation, water table is kept at the ground surface. It should be noted that since the geostatic equilibrium was achieved with a wished in place wall, the bending moment and deflection obtained for piles were induced only due to the excavation.

There are a number of factors which affect the pile group behaviour adjacent to braced excavations. However, this study focuses on the effect of pile configuration, pile cap and distance from the excavation to the pile group on pile group behaviour adjacent to excavations. In this section, shielding effect in pile groups is investigated considering pile bending moments.

Single pile response

In this section, single pile response is explained during progression of the braced excavation. This is important because the group factors are defined in the following sections, with respect to the single pile response during excavations. Figure 11 shows the variation in excavation-induced pile movement in horizontal direction and bending moment along the pile shaft during different stages of the excavation. For the results given in Fig. 11, the pile is located 1.5 m (three pile widths) away from the wall, which is supported by struts having a vertical spacing of 2 m. The first row of struts with a stiffness of 200 MN/m/m was assumed to be fixed at the surface level. The maximum pile deflection changes from 0.9 to 0.7%*H* when the excavation depth, *H*, increases from 4 to 24 m. The maximum deflection of the pile occurs closer to the middle of the pile shaft when the excavation depth is shallow and it moves towards the toe of the pile at the end of the excavation as shown in Fig. 11(a). The deformation profile observed in this study differs from the analysis carried out by Chen and Poulos (1996) and Ong et al. (2006). The main reason for this difference is that in their studies, the excavation depth is shallower than the depth considered in this study. Also, the pile length is shorter than that considered in this study.

Figure 11(b) shows the progression of the bending moment along the pile shaft during the excavation. Maximum bending moment values increase with the depth of excavation, until 12-m depth, and then start to decrease. This is in contrast to the maximum bending moments obtained by Leung et al. (2000) during centrifuge tests for unbraced excavations, where the variation of maximum bending moment with depth is represented as a bilinear variation with continuously increasing maximum bending moment. The reason for this difference is the shallow excavation depth of 4.5 m considered in the centrifuge tests compared to 24-m-deep excavation considered in this study and the unbraced excavation used in the centrifuge test compared to the braced excavation used in this section. After an excavation depth of 12 m, about half of the embedded depth of the pile, the pile started to rotate about its head and this rotation
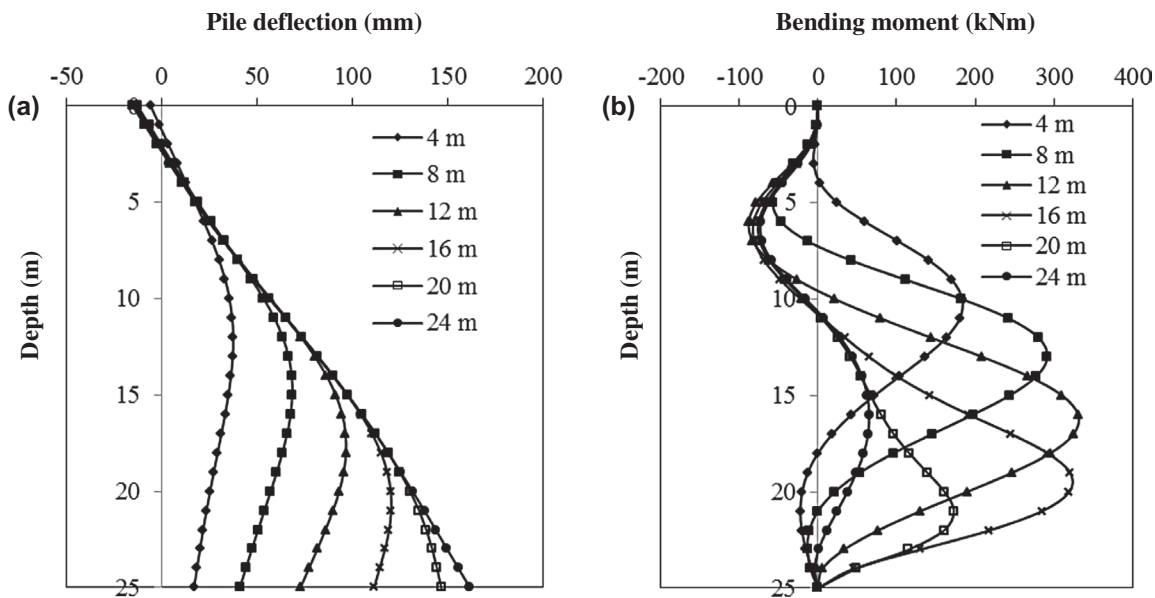
11 *a* Pile deflection and *b* bending moment for single pile located 1.5 m (three pile diameters) from the excavation face

Table 3   Dimensionless maximum pile deflection ($\delta^* = \delta/L$) for single piles at different locations

	Excavation depth/pile length					
Pile location	0.16	0.32	0.48	0.64	0.80	0.96
$X = 3d$	1.48	2.72	3.88	4.80	5.84	6.44
$X = 6d$	1.44	2.64	3.72	4.68	5.68	6.36
$X = 9d$	1.36	2.52	3.56	4.48	5.48	6.24
$X = 12d$	1.28	2.4	3.40	4.28	5.28	6.08
$X = 18d$	1.12	2.16	3.08	3.92	4.84	5.68

Note: d – pile width.

leads to reduction in bending moment developed in the pile. The maximum curvature point in the pile moves towards the toe of the pile and then it starts to move upwards when the excavation depth exceeds 20 m, which is nearly the embedded depth of pile.

Tables 3 and 4 show the dimensionless maximum pile deflections and bending moments induced, respectively, at different stages of the excavation for different pile locations. Pile deflection increases with the excavation depth and decreases with the distance away from the excavation as expected. However, the bending moment values continue to increase only until excavation depth, H, reaches about 48% of the embedded length of the pile, L, and then starts to decrease beyond $H/L = 0.64$ due to the rotation and relaxation of the pile shaft. The increase in bending moment between $0.48 \leq H/L \leq 0.64$ is very small. Therefore, it can be concluded conservatively that the maximum bending moment increases with increase in H up to about 50% of L.

Piles in a group

In this section, the induced maximum bending moments for a pile in a group are studied with respect to a single isolated pile at the same location using the group factor for maximum pile bending moment, m_g, defined as follows (Chen and Poulos 1996):

$$m_g = \frac{\text{Maximum bending moment for a pile when it is in a group}}{\text{Maximum bending moment for a single isolated pile at the same location}} \quad (2)$$

Based on the magnitude of the group factor, we can investigate the shielding effect within the pile group. Also, it can be used to predict the pile group behaviour if the behaviour of a single pile at the same location is known.

Pile group with piles in an infinitely long row adjacent to a braced excavation

Table 5 shows the group factors for bending moments for piles located in a single infinitely long row at different depths of excavation for different centre-to-centre spacings of piles. The row of piles is located 3 m (six times width of the pile) away

**Table 4** Dimensionless maximum pile bending moment ($M^* = ML/EI$) for single piles at different locations

Pile location	Excavation depth/pile length					
	0.16	0.32	0.48	0.64	0.80	0.96
$X = 3d$	0.022	0.035	0.040	0.039	0.021	0.008
$X = 6d$	0.018	0.029	0.034	0.034	0.020	0.008
$X = 9d$	0.014	0.024	0.029	0.029	0.019	0.008
$X = 12d$	0.011	0.019	0.024	0.024	0.017	0.007
$X = 18d$	0.007	0.013	0.016	0.016	0.012	0.006

Notes: d – pile width, L – pile length, I – second moment of area, E – pile Young's modulus and M – maximum bending moment.

Table 5 Group factor for bending moment (m_g) for piles in one infinitely long row

S_h/d	Excavation depth/pile length					
	0.16	0.32	0.48	0.64	0.80	1.00
3	0.97	0.97	0.95	0.94	0.89	0.65
6	1.00	1.00	0.99	1.00	0.99	0.91
9	1.00	1.00	1.00	1.00	1.00	0.99
12	0.99	0.99	1.00	0.99	0.99	1.00

Note: d – pile width.
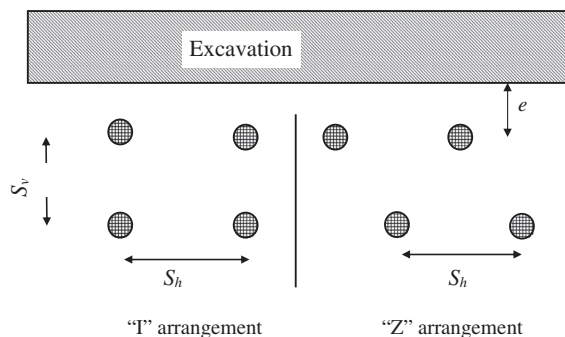
12 Plan view of piles in two infinitely long rows

from the excavation. Group factors for maximum bending moments are close to one, except for the case where piles are located 1.5 m centre-to-centre spacing ($S_h/d = 3$) and the ratio between excavation depth and embedded length of pile (H/L) exceeds 0.8.

Based on these results, the group effect for maximum bending moment is not significant when $S_h/d > 3$. When $S_h/d \leq 3$, group effect is significant for deep excavations, where $H/L \geq 0.8$ and piles in the group experience lower maximum bending moments compared to a single pile in the same location. Since d_g is nearly one for all cases, this reduction in m_g is due to the reduction in pile rotation due to the group effect. In the study presented by Chen and Poulos (1996), when $S_h/d = 4$, they reported m_g of 1.1 and when $S_h/d = 3$, they reported m_g of 1.2. They obtained group factors at the end of a 10-m-deep excavation for a 22-m-long pile, using a two-step approach, where ground deformations due to excavations are computed without incorporating the piles. In addition, H/L ratios considered by them are less than 0.5. However, both studies confirm that the group effect is significant when the $S_h/d \leq 3$, irrespective of the H/L ratio.

Pile group with piles in two infinitely long rows adjacent to a braced excavation

In this section, piles in two parallel rows along the braced excavation are considered. Figure 12 shows the two different pile configurations, i.e. 'I' type and 'Z' type, considered in this study. Table 6 shows the different cases considered with different horizontal (S_h) and vertical (S_v) spacings. In all cases, front row of piles is located 3 m or $6d$ away from the wall.

Table 7 shows the group factors for maximum pile bending moment, m_g. The m_g for both front and rear piles decreases at deeper excavation depths. When the excavation depth is 24 m, Figs. 13(a) and 14(a) clearly shows the shifting and relaxation near the pile tip. Therefore, for both pile group and single pile, bending moments are about four times less when $H/L = 0.96$ ($H = 24$ m) compared to the case when $H/L = 0.16$ ($H = 4$ m). However, a reduction in group factors, m_g, for front piles is observed when H/L exceeds 0.5. When the excavation is deeper ($H/L > 0.5$), according to Fig. 13(a), front pile deformation is nearly the same as for the single pile at the pile tip and pile head. However, the single pile shows higher deformation than the front pile around mid-height and hence maximum bending moment of single pile is higher than the front pile at large excavation depths. Although both single pile and pile group show shifting and relaxation, higher deformation around mid-height of the single pile is due to less rigidity of the single pile compared to the pile group.

The rear piles in the group also show lower m_g at higher excavation depths ($H/L \geq 0.96$) than those for front piles. According to Fig. 14(b), the rotation of the single pile at the location corresponding to the rear pile is less due to the increased distance from the excavation. As a result, for the rear pile, m_g is nearly one up to H/L, *which* is about 0.8. Table 8 shows the group factors for bending moment, respectively, for piles in 'Z' configuration and very similar values are observed as for 'I' configuration. When the spacing S_v shown in Fig. 12

Table 6   Pile configurations for two infinitely long rows

Case	S_h/d	S_v/d
I1	3	3
I2	3	6
I3	6	3
Z1	3	3
Z2	3	6
Z3	6	3

Note: d – pile width.

between piles is increased ($Z1$ to $Z2$), the group factors for displacement and bending moment are almost constant. Although the higher shielding effect is expected when the spacing, S_v, decreases, the distance considered in this analysis does not have much impact on the shielding.

When the horizontal spacing between piles increases, ($Z1$ to $Z3$), the induced bending moment values on front and rear piles decrease when compared to that of single isolated piles. Reduction in the pile group stiffness per unit length leads to higher deformation and lower curvatures.

Two piles in a row perpendicular to the braced excavation face

Here, two piles located in a row perpendicular to the excavation face are considered with and without a pile cap. Different values of e and spacing, s, are considered. Pile cap made of concrete has a cross-sectional area of $(s + 6d)6d$ and a thickness of 1.5 m. Figure 15 shows the variation of deflection along the pile shaft at different depths for front and rear piles for the case, $e = 6d$ and $s = 6d$. Provision of pile cap does not have much influence on the maximum deflection or the deflection profile. The deflection profiles are the same for single isolated pile and the front piles in the group with or without a cap. Rear piles with and without a cap also have the same deflection profile as shown in the Fig. 15(b).

According to Fig. 16, with the provision of pile cap, negative bending moments are developed near the pile cap when the excavation depth is shallower. When the depth increases, negative moments gradually decrease and turn into large positive moments, three times and two times larger than the maximum moment developed in the single isolated pile for front and rear piles, respectively.

Table 7   Group factor for bending moment (m_g) for piles in two infinitely long rows (I)
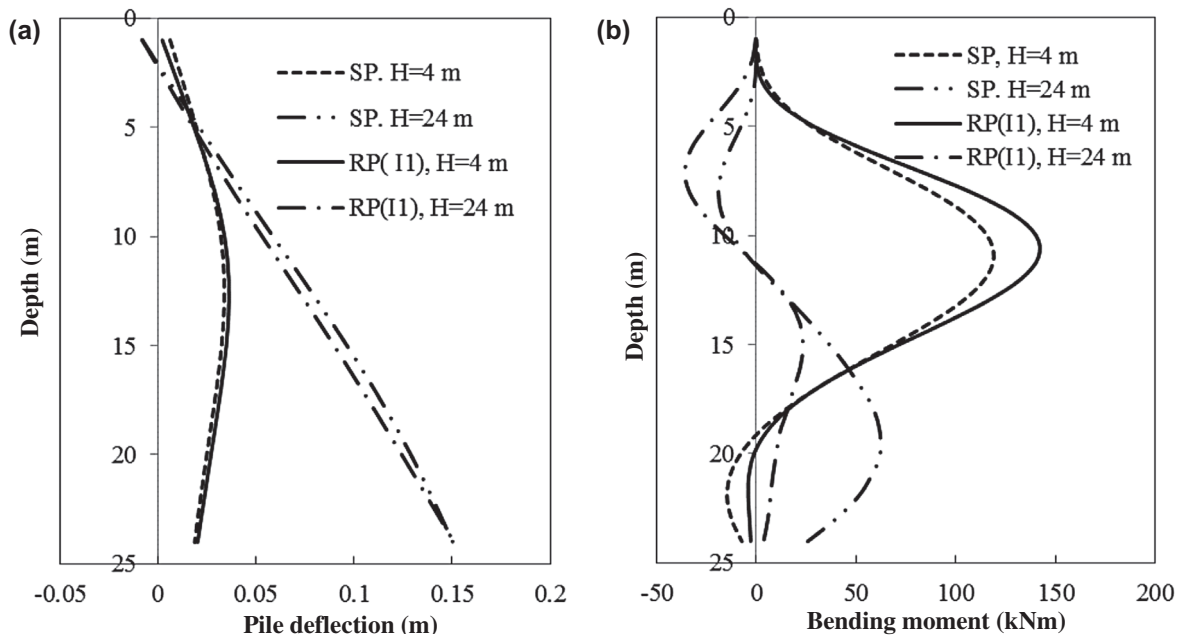
Excavation depth/pile length	Front pile			Rear pile		
	I1	I2	I3	I1	I2	I3
0.16	1.07	1.11	0.91	1.19	1.25	1.01
0.32	1.02	1.04	0.92	1.14	1.20	1.01
0.48	0.95	0.94	0.90	1.06	1.18	1.00
0.64	0.88	0.88	0.84	1.04	1.18	1.02
0.80	0.68	0.72	0.74	0.87	1.01	1.01
0.96	0.90	0.95	0.60	0.57	0.57	0.83
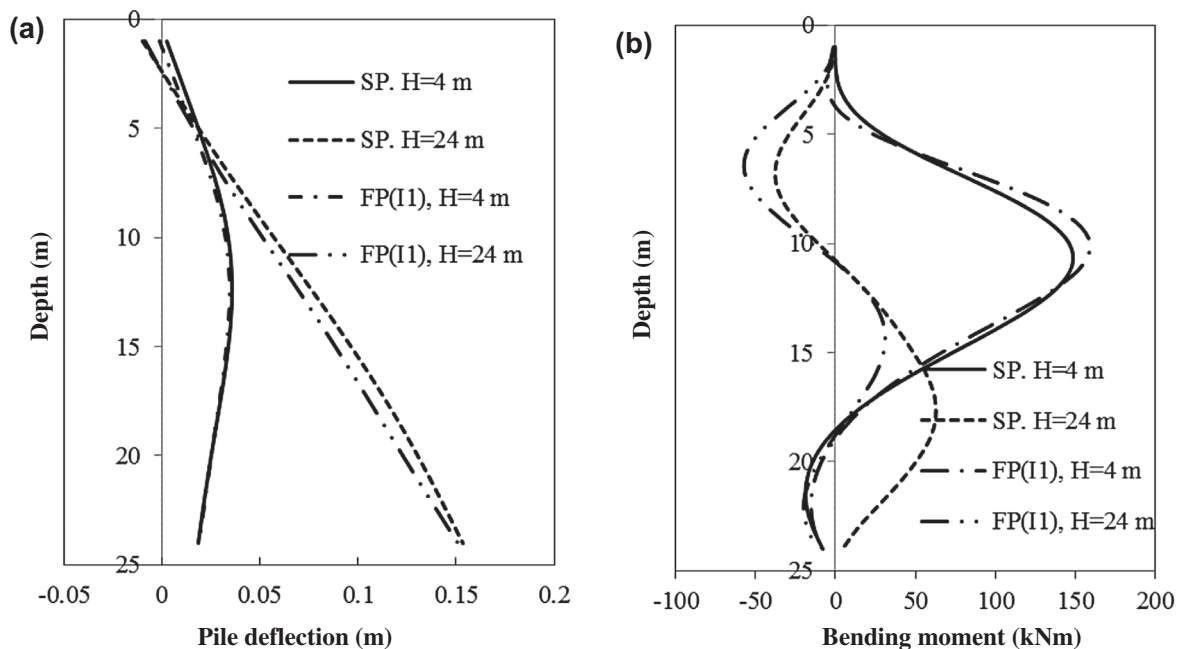
13 *a* Deflection and *b* bending moment profile for single pile ($e = 3$ m) and front pile in 'I1' configuration
Notes: SP – single pile and FP – front pile

14 *a* Deflection and *b* bending moment profile for single pile (*e* = 4.5 m) and rear pile in 'I1' configuration.
   Notes: SP – single pile and FP – rear pile

Table 8   Group factor for bending moment (*m*ₘ) for piles in two infinitely long rows (*Z*)

	Front pile			Rear pile		
Excavation depth/pile length	Z1	Z2	Z3	Z1	Z2	Z3
0.16	1.08	1.11	0.93	1.19	1.25	1.03
0.32	1.02	1.04	0.93	1.14	1.20	1.02
0.48	0.95	0.94	0.91	1.06	1.18	1.01
0.64	0.88	0.88	0.85	1.04	1.18	1.03
0.80	0.68	0.72	0.75	0.87	1.02	1.03
0.96	0.91	0.95	0.60	0.58	0.58	0.85

Table 9   Group factor for bending moment (m_g) for two free-head piles in a row perpendicular to braced excavation
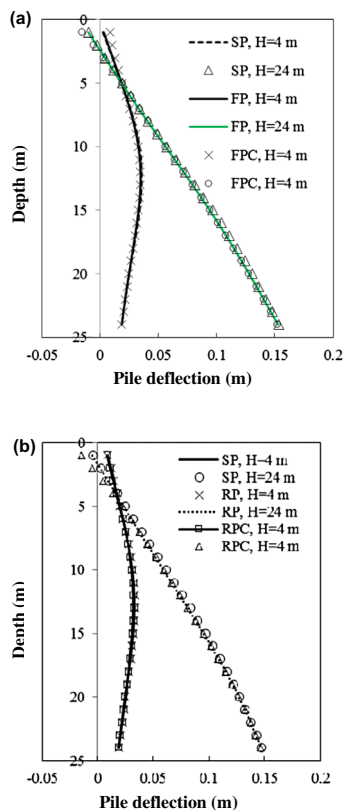
	Front pile			Rear pile		
Excavation depth/pile length	$e=6d, S=3d$	$e=6d, S=6d$	$e=9d, S=3d$	$e=6d, S=3d$	$e=6d, S=6d$	$e=9d, S=3d$
0.16	0.92	0.94	0.92	1.00	1.05	1.01
0.32	0.93	0.95	0.93	1.00	1.05	1.01
0.48	0.92	0.91	0.92	1.00	1.08	1.02
0.64	0.87	0.85	0.85	1.02	1.15	1.06
0.80	0.80	0.82	0.76	1.03	1.17	1.08
0.96	0.73	0.66	0.75	0.95	1.26	1.10

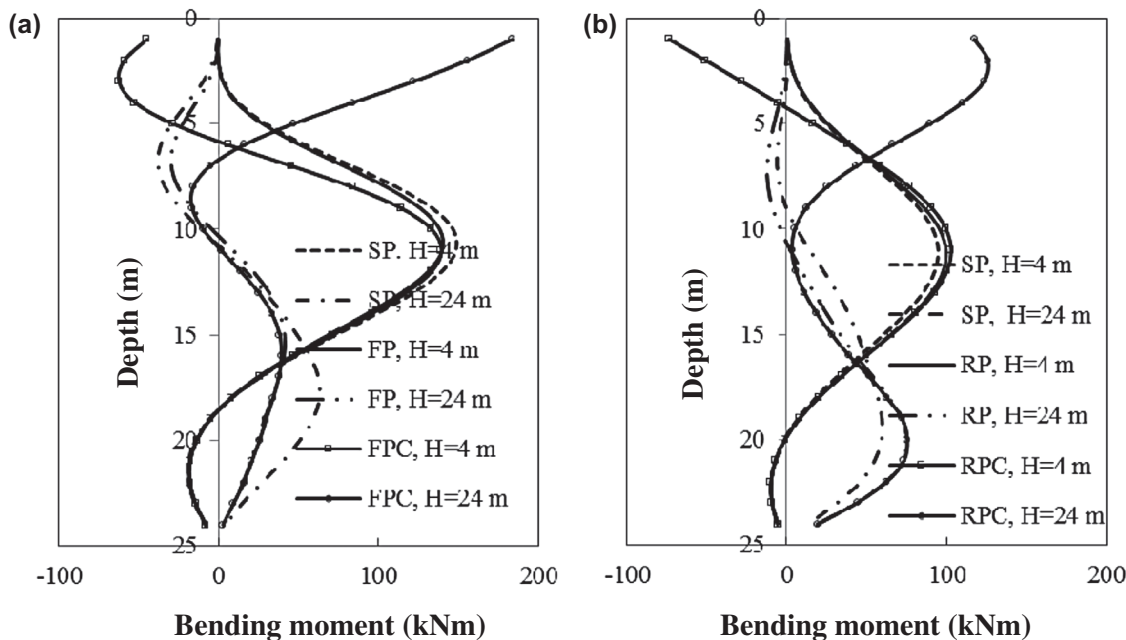Notes: *d* – pile width and *e* – distance from the excavation.

Table 9 shows the group factors for two free-head piles in a row located at different distances from the excavation and different spacings between piles. The bending moment for the front piles is slightly less than that of a single isolated pile due to the additional stiffness caused by the presence of the rear piles. However, the shielding effect of front piles on the rear piles could not be observed. The maximum induced bending moment on the rear piles reduces when the distance between front and rear piles decreases. The maximum induced deflection and bending moment on the front piles do not change with the distance between front and rear piles.

Table 10 shows the group factors for maximum bending moment for the capped piles at different locations with different spacings. The bending moment for the front piles is slightly less than that of a single isolated pile due to the additional stiffness caused by the presence of the rear pile as observed in

15 Deflection profile for *a* front pile and *b* rear pile, (single row of pile perpendicular to the excavation, *e* = 6*d*, S_v = 6*d*).
Notes: SP – single pile, FP – front pile without pile cap, FPC – front pile with the pile cap, RP – rear pile without pile cap and RPC – rear pile with the pile cap

the free-head pile scenario. But substantial amount of positive moments are developed when the braced excavation is deep. This phenomenon differs from the free-head piles, for which the maximum bending moment values are found to be less when compared to that of a single isolated pile at the end of the braced excavation.

Conclusions

In this paper, shielding effect in pile groups adjacent to deep braced and unbraced excavations is investigated using three-dimensional numerical modelling based on the finite element method. The numerical model is validated using a series of centrifuge tests carried out at the National University of Singapore. The results obtained from the finite element analysis showed good agreement with centrifuge test results for the free-head piles. In the case of capped piles, computed bending moments are higher than the measured values due to the difference in degree of pile head fixity developed during the centrifuge tests and numerical modelling. Finally, a parametric study was carried out for both unbraced and braced excavations to investigate the shielding effect in pile groups near excavations.

For the unbraced excavations, results show that:
- The presence of front piles tends to reduce the excavation-induced moments significantly in rear piles.
- In capped-head piles, the maximum lateral movement is less than that of rear piles with a free-head.
- The provision of pile cap helps moderate the excavation-induced lateral movements and maximum bending moments in pile groups at the expense of causing larger negative moments near the pile cap.

For the braced excavations, results show that:

16 Bending moment for *a* front pile and *b* rear pile, (single row of pile perpendicular to the excavation, *e* = 6*d*, S_v = 6*d*)
Notes: SP – single pile, FP – front pile without pile cap, FPC – front pile with the pile cap, RP – rear pile without pile cap and RPC – rear pile with the pile cap

Table 10 Group factor for bending moment (m_g) for two capped-head piles in a row perpendicular to excavation

Excavation depth/pile length	Front pile			Rear pile		
	$e = 6d$, $S = 3d$	$e = 6d$, $S = 6d$	$e = 9d$, $S = 3d$	$e = 6d$, $S = 3d$	$e = 6d$, $S = 6d$	$e = 9d$, $S = 3d$
0.16	0.93	0.94	0.91	1.01	1.08	1.01
0.32	0.94	0.96	0.94	1.01	1.06	1.02
0.48	0.92	0.91	0.93	1.00	1.08	1.03
0.64	0.87	0.85	0.85	1.02	1.15	1.06
0.80	0.81	0.82	0.76	1.03	1.18	1.08
0.96	2.46	2.93	1.60	1.92	2.11	1.17

Notes: d – pile width and e – distance from the excavation.

- For single isolated piles, maximum deflection tends to increase throughout the excavation. Maximum bending moments increase with the depth of excavation, until H/L reaches 0.5 and then tends to decrease due to relaxation near the pile tip.
- For piles in an infinitely long row, the group effect for maximum bending moment is not significant when $S_h/d > 3$. When $S_h/d \leq 3$, group effect is significant for $H/L \geq 0.8$ and piles in the group experience lower maximum bending moments compared to a single pile in the same location.
- For piles in 'I'-type and 'Z'-type configurations, when piles are located in two infinitely long rows, pile configuration does not have much influence on the induced pile behaviour. In both cases, reduction in m_g is observed for front piles when $H/L > 0.5$ and for rear piles when $H/L \geq 0.8$.
- Capped piles tend to develop huge bending moments close to the pile cap. At the end of the excavation, all maximum bending moments developed close to the pile cap are positive and maximum bending moment is up to three times higher than that of a single isolated pile at the same location.
- For the free-head and fixed-head piles, the maximum positive bending moments developed over the lower part of the pile do not have much difference.
- Provision of a pile cap controls the pile head movements of front and rear piles and leads to higher bending at the early and latter stages of the excavation near the pile cap during excavation up to the unsupported depth.

Funding

References

ABAQUS/Standard. 2013. *ABAQUS version 6.11 user's manual*, Providence, RI, Dassault Systèmes Simulia Corporation.

Balachowski, L. 2007. Size effect in centrifuge cone penetration tests. *Archives of Hydro-Engineering and Environmental Mechanics,* **54**, (3), 161–181.

Broms, B. 1979. Negative skin friction, Proceedings, 6th Asian Regional Conference, Soil mechanics and Foundation Engineering, Singapore, 41–75.

Chen, L. T. and Poulos, H. G. (1996). Some aspects of pile response near an excavation. Proceedings, 7th Australia New Zealand Conference on Geomechanics: Geomechanics in a changing world, Barton, ACT: Institution of Engineers, Australia, 1996, 604–609.

Finno, R. J., Lawrence, S. A., and Harahap, I. S. 1991. Analysis of performance of pile groups adjacent to deep excavation. *Journal of Geotechnical and Geoenvironmental Engineering,* **117**, (6), 934–955.

Hashash, Y. M. 1992. Analysis of deep excavations in clay, PhD thesis, Cambridge, MA, MIT.

Huang, J., Han, J., and Oztoprak, S. (2009). Coupled mechanical and hydraulic modeling of geosynthetic-reinforced column-supported embankments. *Journal of Geotechnical & Geoenvironmental Engineering,* **135**, (8), 1011–1021.

Hull, T. S. 1987. The static behaviouf of laterally loaded piles, PhD thesis, Sydney, Australia, School of Civil and Mining Engineering, University of Sydney, Sydney, Australia.

Leung, C. F., Chow, Y. K., and Shen, R. F. 2000. Behaviour of pile subject to excavation-induced soil movement. *Journal of Geotechnical and Geoenvironmental Engineering,* **126**, (11), 947–954.

Leung, C. F., Lim, J. K., Shen, R. F., and Chow, Y. K. 2003. Behaviour of pile groups subject to excavation-induced soil movement. *Journal of Geotechnical and Geoenvironmental Engineering,* **129**, (1), 58–65.

Liang, F., Feng, Y., and Han, J. 2013. A simplified analytical method for response of an axially loaded pile group subjected to lateral soil movement. *KSCE Journal of Civil Engineering,* **17**, (2), 368–376.

Miao, L. F., Goh, A. T. C., Wong, K. S., and Teh, C. I. (2006). Three-dimensional finite element analyses of passive pile behaviour. *International Journal for Numerical and Analytical Methods in Geomechanics,* **30**, (7), 599–613.

Ng, W. W. W., Chan, S. H., & Lam, S. Y. 2005. Centrifuge and numerical modelling of shielding effects on piles in consolidating soil. Proceeding of 2nd China–Japan Geotechnical Symposium, Shanghai, China, 7–19.

Ong, D. E. L. 2004. Pile behaviour subject to excavation-induced soil movement in clay, PhD thesis, National University of Singapore.

Ong, D. E. L., Leung, C. E., and Chow, Y. K. (2006). Pile behaviour due to excavation-induced soil movement in clay I: Stable wall. *Journal of Geotechnical and Geoenvironmental Engineering,* **132**, (1), 36–44.

Ong, D. E. L., Leung, C. E., & Chow, Y. K. 2009. Behavior of pile groups subject to excavation-induced soil movement in very soft clay. *Journal of Geotechnical and Geoenvironmental Engineering,* **135**, (10), 1462–1474.

Potts, D. M. and Zdravkovic, L. 2001. *Finite element analysis in geotechnical Engineering*, London, Thomas Telford.

Poulos, H. G. and Davis, E. H. 1980. *Pile foundation analysis and design*, New York, Wiley.